Radiation Physics and Chemistry 97 (2014) 188–197

Contents lists available at ScienceDirect

Radiation Physics and Chemistry

journal homepage: www.elsevier.com/locate/radphyschem

Study of the optical properties of etched alpha tracks in annealed and non-annealed CR-39 polymeric detectors

A.F. Saad [a,b,*], N.M. Al-Faitory [a], R.A. Mohamed [a]

[a] Physics Department, Faculty of Science, University of Benghazi, Benghazi, Libya
[b] Physics Department, Faculty of Science, Zagazig University, Zagazig, Egypt

HIGHLIGHTS

- UV–visible absorption through etched alpha tracks in annealed and non-annealed PADC films was investigated.
- Films of PADC based NTDs were irradiated with different fluences from alpha particles.
- PADC film samples were annealed at a temperature of 120 °C for durations of 2, 4, 6, 8, and 10 h.
- It is a good method for relative fluence or dose reading.

ARTICLE INFO

Article history:
Received 1 March 2013
Accepted 22 November 2013
Available online 3 December 2013

Keywords:
CR-39 polymer
Alpha tracks
Thermal annealing
UV–visible spectra
Band gap energy
Carbon clusters

ABSTRACT

The UV–visible absorption spectra of virgin and alpha particle-irradiated, annealed and non-annealed CR-39 polymeric track detectors were investigated using a UV–visible spectrometer (Shimadzu mini 1240). Isothermal annealing experiments were carried out on poly allyl diglycol carbonate (PADC) films based nuclear track detectors (NTDs) exposed to a ^{241}Am source. A shifting and broadening of the UV–visible peaks was observed as a result of the etched alpha tracks in the non-annealed and annealed PADC films. The UV–visible spectra of the virgin and non-annealed α-irradiated PADC polymer films displayed a decreasing trend in their optical energy band gaps, both direct and indirect, whereas those measured for the annealed α-irradiated ones showed no significant change. This drop in the energy band gap with increasing fluence is discussed on the basis of the alpha particle- and thermal annealing-induced modifications in the PADC polymeric detector. The results clearly showed that the values for the indirect energy band gap were lower than the corresponding values for the direct band gap. In addition, the Urbach energy was estimated from the Urbach edge, and exhibited roughly the same trend as the optical band gap. Finally, this study presents new results showing that the annealed PADC films were highly insensitive to alpha particles.

1. Introduction

The science of polymer based solid state nuclear track detection (SSNTD) has come a long way since its birth in 1963 in high polymers (Fleischer and Price, 1963), when these materials served as simple detectors of heavily charged particles. In fact, the discipline called SSNTD dates back to 1958 and its roots in the United Kingdom (Young, 1958). The importance of the poly allyl diglycol carbonate (PADC) polymer, known commercially as CR-39, and its use as a solid state nuclear track detector SSNTD, began when two scientific groups independently published two papers within a short space of time (Cartwright et al., 1978; Cassou and Benton, 1978). During the subsequent three decades, this polymer was applied to the fields of nuclear and particle physics, cosmic rays and high energy interactions, plasma physics, environmental and earth sciences, dosimetry and radiation protection, radiation-induced material modifications and other technological sciences. Thus, the photon (Saad et al., 2005; Sharma et al., 2007; Zaki, 2008; Raghuvanshi et al., 2012), neutron (Khan et al., 2005; Kumar et al., 2010; Kumar et al., 2011) and charged particle (Phukan et al., 2003; Lounis-Mokrani et al., 2003; Yamauchi et al., 2005) irradiation of polymeric detector materials is an interesting method of significantly altering the physical, chemical, structural, optical, mechanical and electrical properties of polymeric materials. In general, charged particles passing through matter deposit energy in the detector material and cause irreversible modifications of the macromolecular structure of the detector material (Marletta, 1990;

* Corresponding author at: Physics Department, Faculty of Science, University of Benghazi, Benghazi, Libya. Tel.: +218 92 8128608; fax: +218 61 2229617.
E-mail address: abdallahsaad56@hotmail.com (A.F. Saad).

0969-806X/$ - see front matter © 2013 Elsevier Ltd. All rights reserved.
http://dx.doi.org/10.1016/j.radphyschem.2013.11.021

Calcagno et al., 1992; Abel et al., 1995; Saad et al., 2012). Alpha particles, being electrically charged, deposit energy through electrical interaction with the atomic electrons in the detector and create, along their ionization trajectory, a region that is more sensitive to chemical etching than elsewhere in the bulk. After treatment with an aggressive etching solution, the tracks remain as holes or pits and their size and shape can be measured. The temperature is another crucial parameter affecting PADC films. High temperatures may cause considerable disorder in the spacing between the constituent molecules of these PADC films. This was demonstrated in our previous study, where thermal annealing induced significant modifications in the registration properties of charged particles in PADC films based on NTDs (Saad et al., 2012). The effects of thermal annealing on nuclear tracks in solids have already been studied by many other researchers (Fleischer et al., 1964; Modgil and Virk, 1985; Ipe and Ziemer, 1986; Salamon et al., 1986; Durrani et al., 1990; Abou El-Khier et al., 1995; Anupam and Kumar, 1997; Jain et al., 1998; Rana et al., 2000; Rana, 2012; Jain et al., 2012). As a fine tool for our study, we introduced UV–visible spectroscopy to make direct observations of the modifications to the optical properties along the etched alpha tracks in annealed and non-annealed PADC polymeric detectors.

2. Materials and experiments

PADC polymer sheets of TASTRAK were produced and provided by Track Analysis Systems Ltd. (TASL), Bristol, UK. The standard thickness of 750 μm was used. The polymeric detector samples for the current study were cut to a size of 2×2 cm^2. The samples were irradiated (in contact) using a planar ^{241}Am source with an activity 1.3×10^5 Bq. Two sets of detectors were prepared for these experiments; one for the non-annealed experiments, and the other for the annealed experiments. In addition, one virgin sample was kept as a control. Prior to being exposed to the radiation or annealing, the protective cover of polyethylene was removed. The irradiation was performed in air, using 2π geometry. The irradiation periods were 1, 5, 10, 15, 20 and 25 s. The CR-39 detectors were annealed in a temperature-controlled oven for different time intervals, at a temperature of 120 °C. The first set of CR-39 detectors was exposed to α-particles but not annealed, to allow a comparison with the results from the annealed detectors. The second set was first annealed in the oven, and then irradiated with α-particles (exposure post-annealing). After the exposure, the detectors were chemically etched in a 6.25-M solution of NaOH at 70 ± 1 °C for different etching interval times. Then the detectors were washed in distilled water in order to stop the chemical reaction and also to avoid contamination by the etching solution on the surface of the detector material. The detectors were read and the density of the tracks was counted using an optical microscope with appropriate magnification.

The virgin, alpha irradiated and annealed/alpha irradiated PADC polymer samples were subjected to spectral studies in the Ultraviolet and Visible region. These studies were carried out using a UV–visible Spectrophotometer (Shimadzu mini 1240) in the wavelength range 190–900 nm at the scanning speed of 25 nm/min.

3. Results and discussion

3.1. Measurement of absorbance through the etched alpha tracks in annealed and non-annealed CR-39 NTDs

For ionizing particles, the radiation energy was deposited locally along the track for both sets (non-annealed and annealed) of CR-39 plastic detectors. As a typical example, the UV–visible absorption spectra of non-annealed and annealed CR-39 NTDs exposed to alpha particles are shown in Fig. 1. This figure shows the effect of isothermal annealing for 2, 4, 6, 8, and 10 h at 120 °C on the optical absorption of α-particle-irradiated PADC films, where the exposure was performed post-annealing. It is worth mentioning that the optical spectra show an increase and a shift of absorption edge towards longer wavelength with increasing alpha fluence in the non-annealed PADC films as seen in Fig. 1-(a), while the UV spectra for the annealed films show the opposite effect with increasing annealing time as also seen in the same figure from (b) to (f). This indicates a decline in the band gap after alpha exposure and chemical etching in the non-annealed PADC films, while this decline was observed to only a small degree in the annealed films, especially at longer annealing times. This decline was generally attributed to the formation of extended systems of conjugate bonds such as C=C or C=O, as a result of the alpha particle- or heavy ion-induced bond cleavage and reconstitution, which generated some chromophoric groups (Phukan et al., 2003; Saha et al., 2000). Furthermore, the increasing intensity of the shoulder peak at approximately 280 nm with the increases in fluence was assigned to the $[R–C=C–OH]_n$ groups in the conjugated system; this confirmed the creation of OH groups in gamma-, proton-, and heavy ion-irradiated PADC films, as shown using FTIR analysis (Saad et al., 2005; Lounis-Mokrani et al., 2003; Yamauchi et al., 2005). We also observe broadening of the absorption peak with increasing fluence for the non-annealed detectors. This broadening can be attributed to the production of defects induced by the ionizing radiation. These defects may result from the formation of new energy levels causing the broadening of the absorption peaks. It should be noted that the UV–vis spectra show a systematic enhancement of absorbance of the 250–850 nm band with increasing alpha fluence. Such fluence dependence of the spectra should be directly related to the chemical changes in the structure of the damage trails in the PADC polymer films. This fluence dependence of the spectra is actually attributed to the excitation of π electrons due to the formation of carbon clusters; this requires only a small amount energy, which can be provided by the ionizing alpha particle, and hence transitions of this type occurs in this band. In contrast, in the annealed films, this broadening of the absorption peak significantly decreased with increasing annealing time. In this case, the absorption peak resembled the one observed for the virgin PADC film. Overall, the isothermal annealing process tended to decrease the alpha track density, until they completely disappeared at longer annealing times. PADC films typically suffer serious degradation under annealing with these temperatures and annealing times. The surface material of the PADC film then becomes permanently softened, producing an increase in the bulk etch rate representing the degree of softening, which results in a decrease in the detection sensitivity and the detection thresholds for α-particles as seen in Table 1. This means that annealed PADC films become rather insensitive to particles with lower ionization rates – e.g., α-particles – compared with heavily ionizing particles (e.g., fission fragments) (Saad et al., 2012).

3.2. Calculation of the Urbach energy

Electrons are excited between the bands of a solid material via optical transitions. The optical absorption coefficient $\alpha(h\nu)$ is defined as a fraction of the power absorbed in a unit length of the solid. The absorption coefficient $\alpha(h\nu)$ can be calculated from the absorbance (A) by using the following formula (Fox, 2001)

$$\alpha(h\nu) = A/l \quad (1)$$

where l is the sample thickness in cm and A is defined as $A = \log(I_o/I)$, where I_o and I are the intensity of the incident

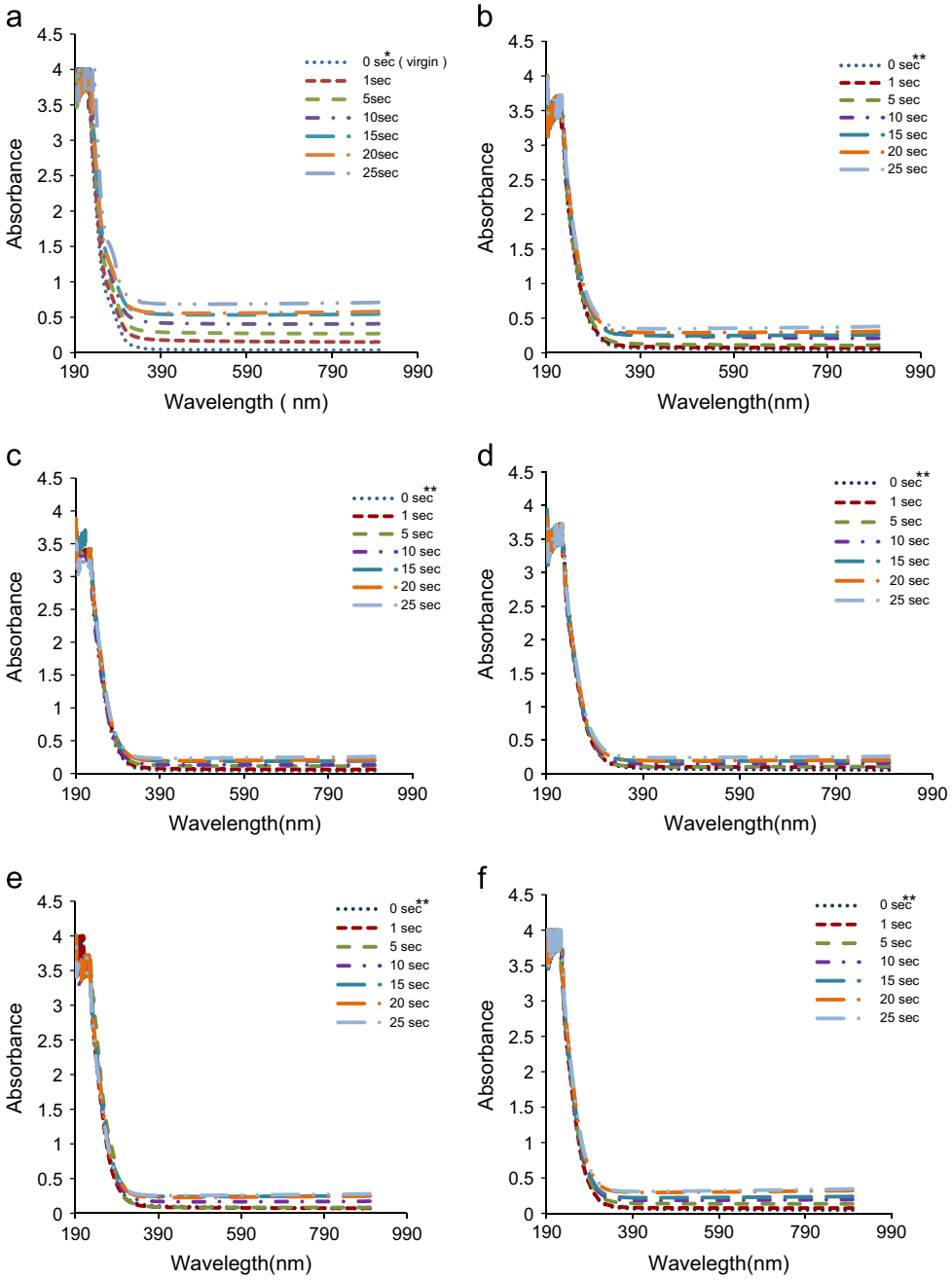

Fig. 1. UV–visible spectra of the non-annealed and annealed PADC film-based NTDs exposed to alpha particles for irradiation periods of 1, 5, 10, 15, 20 and 25 s. The thermal annealing was performed at 120 °C for durations of 2, 4, 6, 8, and 10 h, respectively. * indicates non-annealed and un-irradiated film which means a virgin one, while the other non-annealed films in (a) exposed to alpha particles with different fluences. ** indicates the un-irradiated and annealed ones for durations of 2, 4, 6, 8, and 10 h as depicted in (b), (c), (d), (e) and (f), respectively.

Table 1
Values of annealing time, bulk and track etch rates V_B and V_T, sensitivity $V=V_T/V_B$ and increase of V_B in percentage (the degree of softening).

Annealing time	V_B (μm/h)	V_T (μm/h)	V	Increase of V_B in percentage (the degree of softening)
0	1.35	3.46	2.58	–
2	1.60	3.66	2.29	18.5
4	1.68	3.54	2.11	24.4
6	1.75	3.62	2.07	29.6
8	2.25	4.25	1.89	66.7
10	2.28	4.01	1.76	68.9

and transmitted UV–visible beams, respectively. The absorption coefficient is very small below the band edge in insulators whereas, in other materials, e.g. semiconductors, it is found to vary exponentially with the photon energy ($h\nu$) which follows the Urbach relation (Urbach, 1953)

$$\alpha(\nu) = \alpha_o \exp(h\nu/E_u) \quad (2)$$

where $\alpha(h\nu)$ is the absorption coefficient, which is a function of photon energy $h\nu$. α_o is a constant and E_u, Urbach's energy, is equal to the inverse logarithmic slope of the absorption coefficient. This Urbach's energy originates from the thermal vibrations in the lattice of silver halides for a direct band gap system (Urbach, 1953).

The logarithm of the absorption coefficient $\alpha(h\nu)$ as a function of the photon energy ($h\nu$) for the non-annealed and annealed films, for different durations at 120 °C, PADC films after irradiation with different fluences of alpha particles are plotted in Fig. 2. The values of the Urbach energy (E_u) are calculated by taking the reciprocal of the slopes of the linear portion in the lower photon energy region of these curves and are listed in Table 2. The results show that the E_u values increase as the alpha fluence increases and this may be attributed to the enhancement of damage trails in the non-annealed PADC films. In contrast, in the annealed films, no significant effects of the E_u values were observed from 2 to 8 h of annealing, but for 10 h of annealing, more or less constant significant variations in the overall fluences of the α-particle exposure were observed. This might have been due to the significant transformations taking place in these polymer materials that were induced by the different types of radiation, and the nature of the target material itself; the changes in the polymer materials occurred in both the parameters and structure (for example, the energy, LET, fluence, and mass). The thermal annealing, on the other hand, induced negative changes in the registration properties of the charged particles with a lower ionization rate (i.e., the α-particles). It should be noted that the non-annealed results were not consistent with the published data for gamma and neutron irradiation for Ultra-high-molecular-weight-polyethylene (UHMWPE) and PADC polymer (Zaki, 2008; Raghuvanshi et al., 2012; Kumar et al., 2011), since these results show that the Urbach energy was reduced with gamma dose or neutron fluence. In the current study, the Urbach energy shows

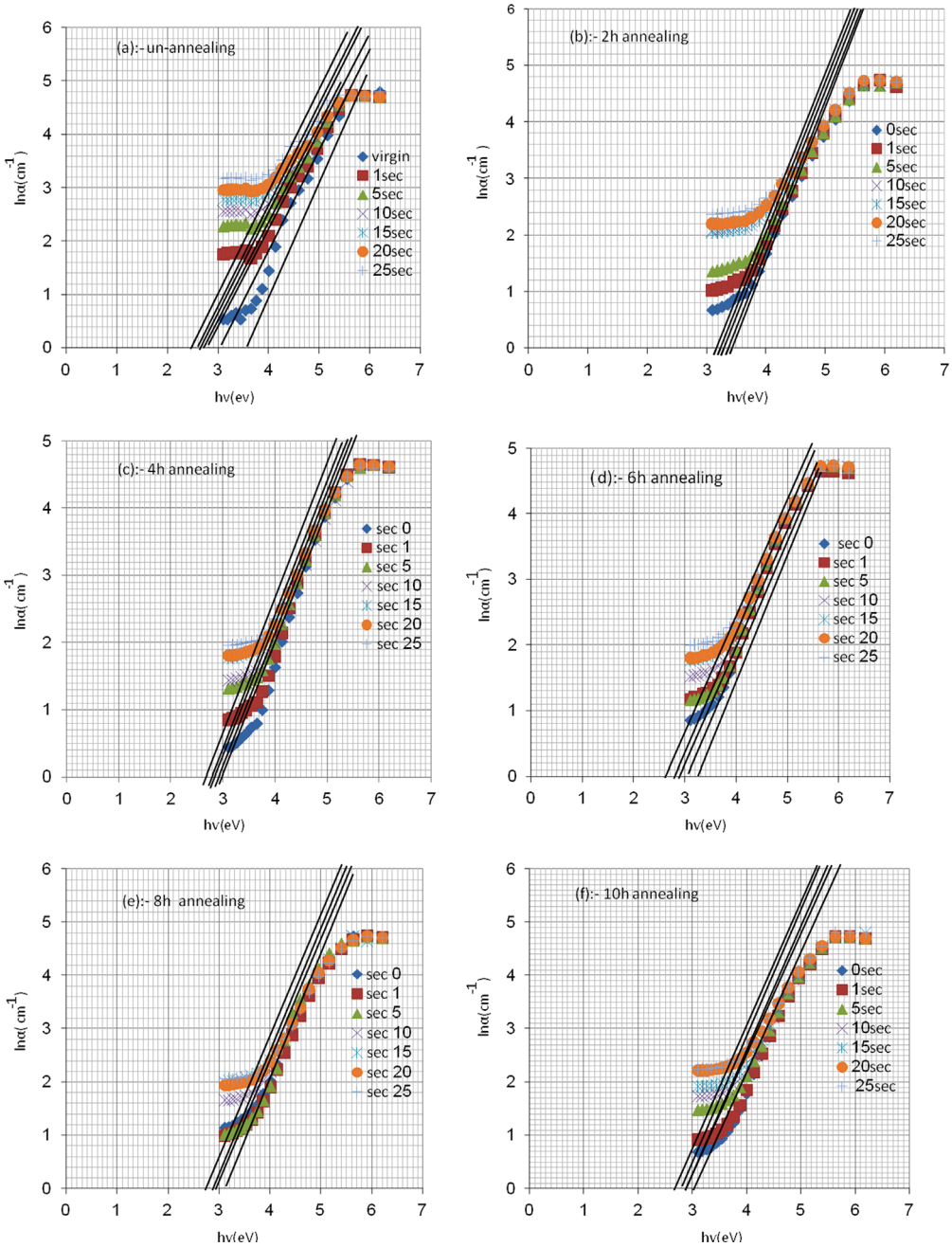

Fig. 2. Logarithmic variation of the absorption coefficient $\alpha(h\nu)$ as a function of photon energy ($h\nu$), for the non-annealed and annealed PADC films exposed to alpha particles with different fluences. The solid linear lines stand for the fitting lines of the straight parts of the curves to the energy axis ($h\nu$). The values of the Urbach energy are determined by taking the reciprocal of the slopes of theses linear lines.

Table 2
Optical band gap energy, phonon energy, Urbach energy, and carbon atoms (N) in a cluster of non-annealed and annealed PADC polymer-based NTDs irradiated by alpha particles with different fluences. Thermal annealing was performed at a temperature of 120 °C for durations of 2, 4, 6, 8, and 10 h.

Annealing time	Alpha fluence (s)	Band gap energy (eV)		Phonon energy (eV)	Urbach energy (eV)	Carbon atoms (N) in a cluste	
		Indirect	Direct			Indirect	Direct
0	0[a]	3.53	4.90	1.37	0.45	5	3
	1	3.33	4.85	1.52	0.55	5	3
	5	3.00	4.75	1.75	0.56	6	4
	10	2.82	4.75	1.93	0.58	6	4
	15	2.72	4.65	1.93	0.59	7	4
	20	2.62	4.65	2.03	0.60	7	4
	25	2.42	4.55	2.13	0.61	8	4
2	0	3.50	4.80	1.30	0.47	5	4
	1	3.45	4.75	1.30	0.48	5	4
	5	3.45	4.75	1.35	0.47	5	4
	10	3.35	4.70	1.35	0.47	5	4
	15	3.35	4.70	1.35	0.47	5	4
	20	3.3	4.65	1.35	0.48	5	4
	25	3.25	4.65	1.40	0.48	5	4
4	0	3.70	4.87	1.17	0.46	5	4
	1	3.65	4.85	1.20	0.45	5	4
	5	3.60	4.83	1.23	0.44	5	4
	10	3.55	4.80	1.25	0.44	5	4
	15	3.50	4.78	1.28	0.44	5	4
	20	3.50	4.75	1.25	0.44	5	4
	25	3.50	4.75	1.25	0.43	5	4
6	0	3.80	4.88	1.08	0.50	5	4
	1	3.80	4.88	1.08	0.50	5	4
	5	3.80	4.88	1.08	0.50	5	4
	10	3.75	4.84	1.09	0.46	5	4
	15	3.70	4.80	1.10	0.47	5	4
	20	3.70	4.80	1.10	0.47	5	4
	25	3.65	4.76	1.11	0.50	5	4
8	0	3.60	4.70	1.10	0.45	5	4
	1	3.60	4.70	1.10	0.45	5	4
	5	3.60	4.60	1.00	0.45	5	4
	10	3.55	4.65	1.10	0.46	5	4
	15	3.50	4.65	1.15	0.46	5	4
	20	3.45	4.65	1.20	0.46	5	4
	25	3.45	4.65	1.20	0.46	5	4
10	0	3.5	4.80	1.30	0.60	5	4
	1	3.45	4.80	1.35	0.60	5	4
	5	3.40	4.75	1.35	0.60	5	4
	10	3.35	4.75	1.40	0.63	5	4
	15	3.30	4.70	1.40	0.63	5	4
	20	3.25	4.65	1.40	0.60	5	4
	25	3.25	4.60	1.35	0.60	5	4

[a] PADC film is virgin.

the opposite trend for the non-annealed alpha-irradiated PADC films, but it changed almost insignificantly in the annealed exposed films, compared with the virgin film, except at 10 h.

3.3. Determination of band gap: direct and indirect transitions

The relationship mentioned above was first proposed by Urbach (Urbach, 1953) to describe the absorption edge in alkali halide crystals although it has been found to hold for many amorphous materials. Eq. (2) has been modified to a more general form by Mott and Davies (1979).

$$\alpha(h\nu) = B(h\nu - E_g)^n / h\nu \tag{3}$$

where $h\nu$ is the energy of the incident photons, the factor B depends on the transition probability and can be assumed to be constant within the optical frequency range, and E_g is the value of the optical energy gap between the valence band and the conduction band and n is the power, which characterizes the electronic transition, whether it is direct or indirect during the absorption process in K-space. Specifically, $n$is 2, 3, 1/2 and 3/2 for indirect allowed, indirect forbidden, direct allowed and direct forbidden transitions, respectively. In the case of the direct energy band gap, the optical transition due to excitation of electrons between the lower band and upper band takes place directly, whereas in the indirect one the relative positions of the conduction band and valence band do not match and the transition involves phonons in order to conserve momentum (Fox, 2001). The phonon energy ε can be calculated from the energy difference between the optical band gap energy transitions (direct, E_g^d, and indirect, E_g^{ind}) using the following formula:

$$\varepsilon = E_g^d - E_g^{ind} \tag{4}$$

From the UV–visible absorption spectra, the band gap of the non-annealed and annealed PADC polymer films, followed by alpha exposure and chemical etching, was calculated by extrapolation of the plot of $(\alpha h\nu)^{1/n}$ versus $(h\nu)$ on the $h\nu$ axes. For the determination of indirect and direct energy band gap, $(\alpha h\nu)^{1/2}$ and $(\alpha h\nu)^2$, respectively, were plotted as a function of photon energy $(h\nu)$, taking into account the linear portion of the fundamental absorption edge of the UV–visible spectra, as shown in Fig. 1. These plots are presented in Figs. 3 and 4, respectively. From the intercept of the fit lines, the fitting was somewhat low for some data, on the $h\nu$ axis as depicted in Figs. 3 and 4, the indirect and direct band gaps have been determined for virgin and alpha-irradiated, annealed and non-annealed PADC polymer films with different fluences. The results are presented in Table 2. It can be seen that the band gap for the non-annealed PADC film based NTDs decreases from 3.53 to 2.42 and 4.9 to 4.55 eV for indirect and direct transitions, respectively, as a result of alpha irradiation. The same band gap for the annealed α-exposed ones decreased from 3.50 to 3.25, 3.70 to 3.50, 3.80 to 3.65, 3.60 to 3.45 and 3.50 to 3.25 eV, and from 4.80 to 4.65, 4.87 to 4.75, 4.88 to 4.76, 4.70 to 4.65 and 4.80 to 4.60 eV, corresponding to annealing times of 2, 4, 6, 8, and 10 h for the indirect and direct transitions, respectively. The variation of optical band gap with alpha irradiation can be explained as the drastic change in the degree of disorder due to the fact that alpha particles create along their path a region of damage trails produced by three processes, physical, physico-chemical and chemical (Durrani and Bull, 1987). Such trails are more sensitive to etching solution than the rest of the bulk material of PADC polymer based NTDs, so these etched damage trails, called etch pits or tracks, display the increasing disorder in the detector material (Fleischer et al., 1975). The decline of the band gap of the non-annealed PADC polymer is attributed to the amount of disorder in the polymer because the light transmittance depends on track density and alpha energy, as well as the etching and storage conditions of the detector material (Yamauchi et al., 2005; Saad et al., 2011). The effects of the annealing on the optical band gap energy and indirect and direct transitions in the PADC film material exposed to particles with lower ionization rates (such as α-particles) were also determined for different fluences, as shown in Table 2. The annealing mechanism and characteristics of the optical band gap energy, and the indirect and direct transitions of α-particle tracks in CR-39 PADC films are illustrated in Fig. 5. Here, we focus on the annealing characteristics of α-particle tracks in CR-39 PADC films; a change in annealing time should produce a change in the optical band gap energy. However, after an annealing time of approximately 6 h, a detector material will begin to approach a maximum band gap energy. The annealing results showed two regimes with clearly different annealing rates. In the first regime, the annealing rate was high, whereas in

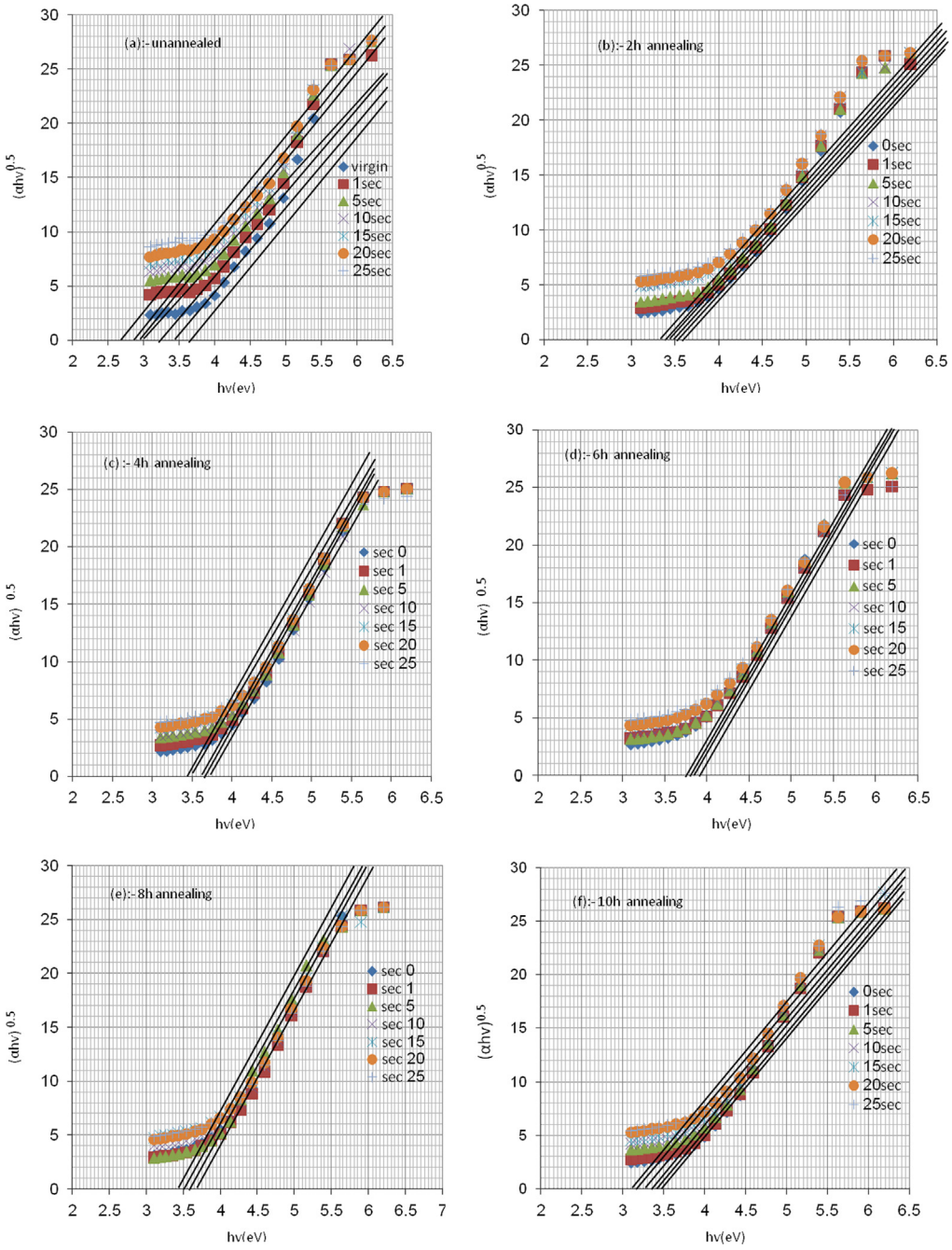

Fig. 3. Plots for indirect band gap (eV) in non-annealed and annealed PADC films exposed to alpha particles with different fluences. The solid linear lines stand for the fitting lines of the straight parts of the curves to the energy axis ($h\nu$). The extrapolation of these solid linear lines to the energy axis ($h\nu$) yields the indirect band gaps.

the other region, the rate was somewhat low, or close to constant. Similar behavior was observed recently by Rana (2012), but the annealing time intervals were not long enough, ranging from 5 to 30 min; in the present investigation, the thermal annealing was severe, because the annealing times were too long (ranging from 1 to 10 h), as reported in our previous study (Saad et al., 2012).

Fig. 6 shows the phonon energy ε dependence of the α-particle fluence applied to the non-annealed and annealed polymer PADC film-based NTDs, for different annealing times ranging from 2 to 10 h. With increasing α-particle exposure, the phonon energy at 0 h (no annealing) increased linearly, while from 2 to 10 h the phonon energy values remained almost constant. These values were far lower than that those of the non-annealed PADC films. The phonon energy steadily decreased as the annealing time was varied from 2 to 8 h, for all α-particle fluences, but for times longer than 10 h it increased again. The large variation in the phonon energy values between the non-annealed and annealed films for all α-particle fluences might have resulted from the formation of double bonds with the conjugated system in the alpha-exposed PADC film; this phenomenon can also result in the generation of chromophoric groups (Lounis-Mokrani et al., 2003; Saad et al., 2005). On the other hand, the phonon energy ε generated after every transition induced in the non-annealed PADC films (in the case of the indirect transition) showed increases in its value with increases in the fluence, while in the annealed films it showed the opposite effect.

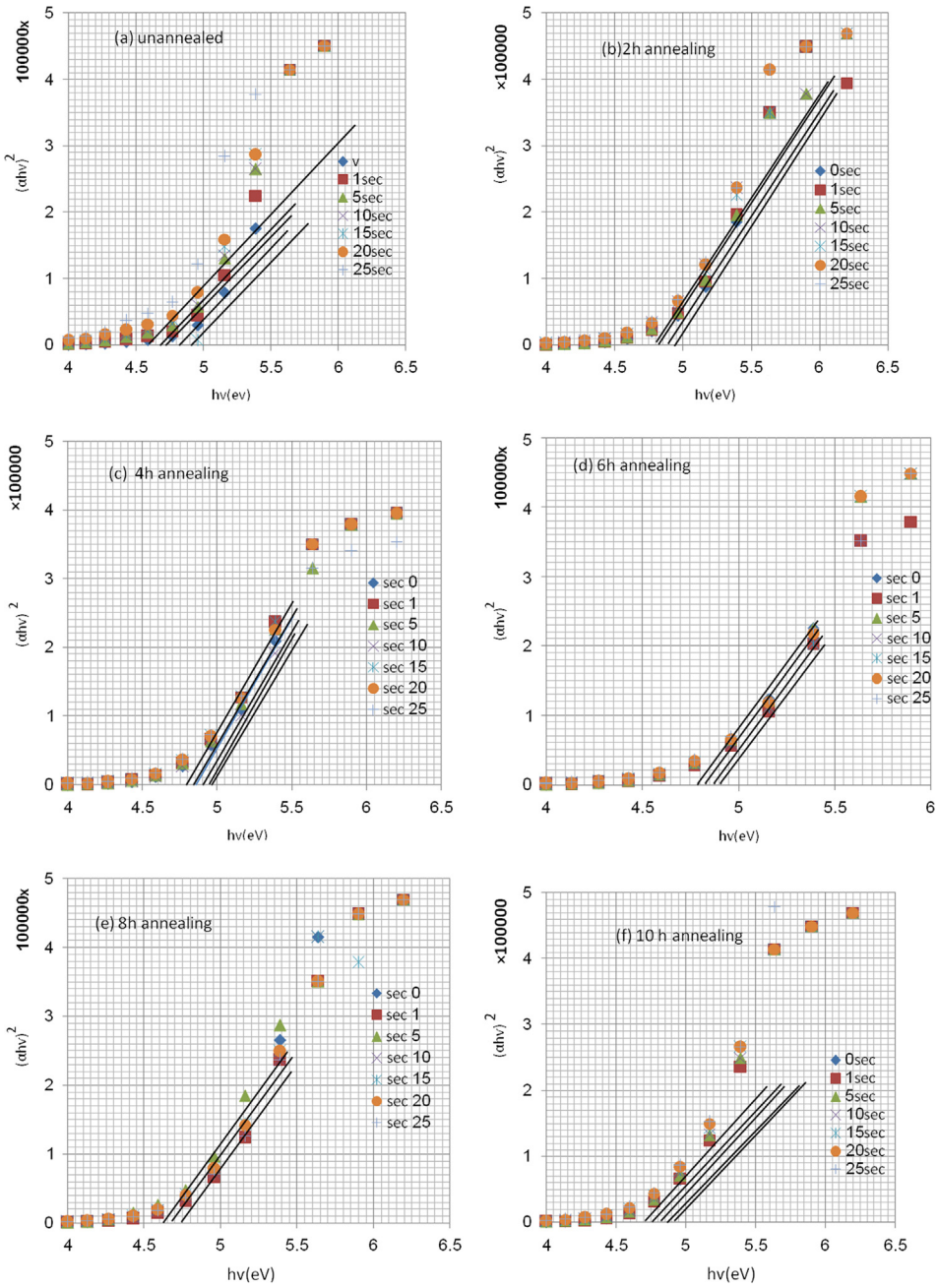

Fig. 4. Plots for direct band gap (eV) in non-annealed and annealed PADC films exposed to alpha particles with different fluences. The solid linear lines stand for the fitting lines of the straight parts of the curves to the energy axis ($h\nu$). The extrapolation of these solid linear lines to the energy axis ($h\nu$) yields the direct band gaps.

3.4. *Estimation of the number of carbon atoms in a cluster*

For a linear structure, the number of carbon atoms per conjugation length N (Fink et al., 1995) is given by

$$N = 2\beta\pi/E_g \tag{5}$$

where N is the number of carbon atoms per conjugated length and 2β gives the band structure energy of a pair of adjacent π sites. The value of β is taken to be -2.9 eV as this is associated with the $\pi \rightarrow \pi^*$ optical transition in the –C═C– structure. The results of the number of carbon atom (N) values per conjugation length, known as a cluster, are given in Table 2. It can be seen that the number of carbon atoms per cluster increases with increase in the exposure time for alpha particles irradiating the non-annealed PADC films, whereas for the annealed/α-particle-exposed films, the number of carbon atoms remained constant. Moreover, the number of carbon atoms per cluster for the indirect band gap energy is relatively high compared with the direct band gap for virgin and etched PADC polymer film based NTDs irradiated by alpha particles with different fluences.

4. Conclusion

The analysis of the UV–visible spectra of alpha-irradiated, non-annealed and annealed PADC film-based NTDs led to the following conclusions:

(1) Alpha particle irradiation had a significant effect on the optical band gap energy, and direct and indirect transitions, of

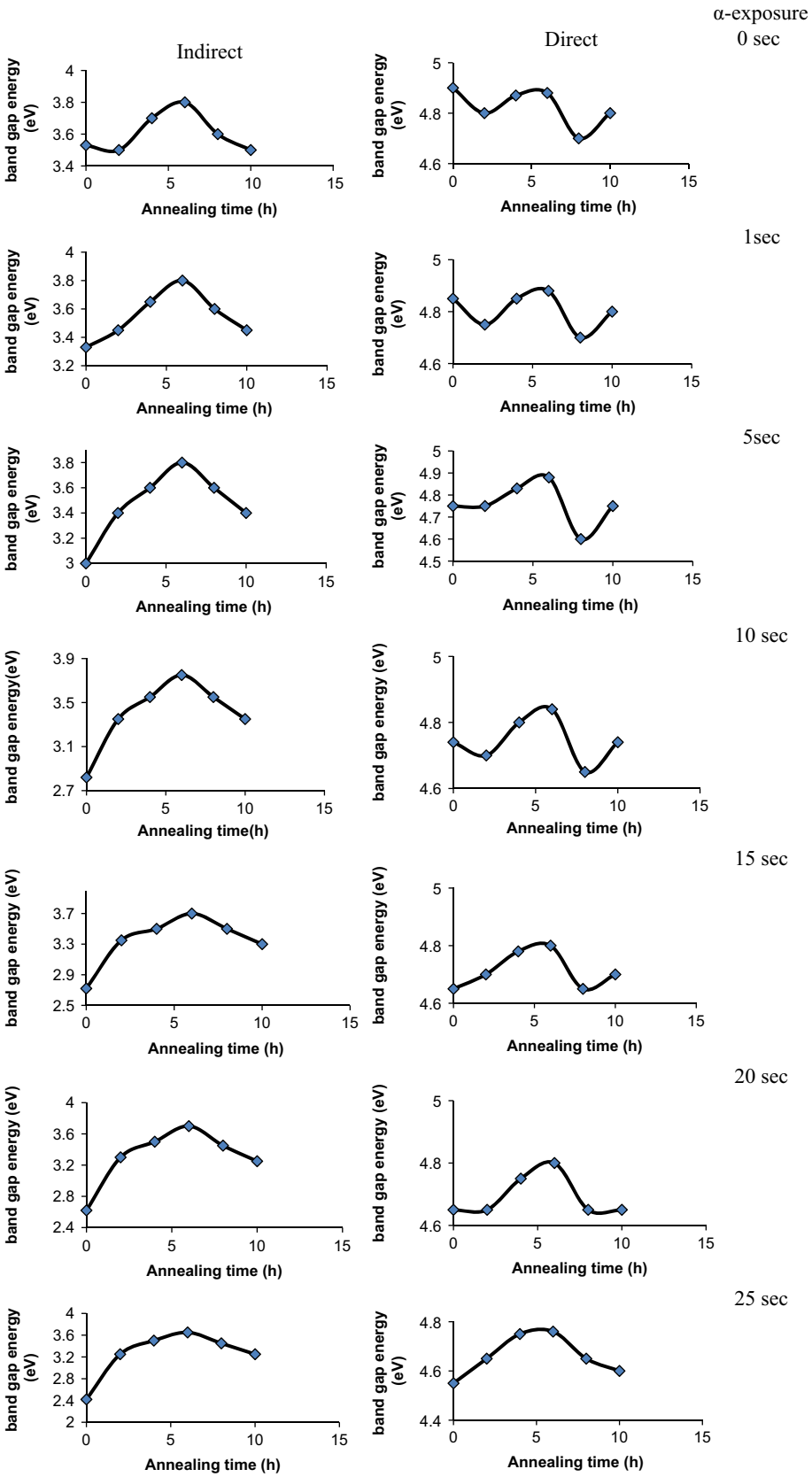

Fig. 5. Variation of the optical band gap energy, for indirect and direct transitions, as a function of annealing time; the annealing was performed at 120 °C, on non-annealed and annealed PADC films exposed to alpha particles with different fluences.

the non-annealed PADC films. The alpha particles also induced the formation of some chromophoric groups, which was attributed to the formation of C═O and C═C conjugated systems of bonds. Decreases of 31.4 and 7.1% were observed in the energy band gaps for the virgin PADC film and the alpha-irradiated PADC based CR-39 NTDs, from 3.53 and 4.9 eV to

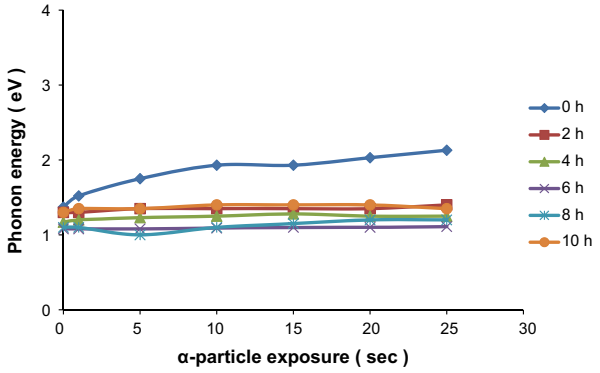

Fig. 6. Variation of phonon energy as a function of alpha particle fluence in non-annealed and annealed PADC films. The thermal annealing was performed at 120 °C for durations of 2, 4, 6, 8, and 10 h, respectively.

2.42 and 4.55 eV, respectively, for indirect and direct transitions. Large increases of 55.5 and 35.6% were observed in the phonon energy and Urbach energy for the virgin film and the irradiated film, from 1.37 and 0.45 eV to 2.13 and 0.61 eV, respectively; this might have been due to the amorphization of the PADC film after alpha particle exposure. Also, increases of 60 and 33.3% in the number of carbon atoms (N) per conjugated length, the cluster size, from 5 and 3 to 8 and 4 for the virgin film and the irradiated film, in both transitions, indirect and direct, respectively. Overall, the optical absorption data indicated a progressive closure of the optical band gap as the ion fluence increased. The optical transitions of $\pi \rightarrow \pi^*$ in the –C═C– structure played an interesting role in the latent track formation in the PADC film in the low-energy range.

(2) Thermal annealing induced considerable changes in the optical properties of the PADC films. Decreases of 7.1 and 3.1, 5.4 and 2.5, 3.9 and 2.5, 4.1 and 1.1 as well as 7.1 and 4.2% in the energy band gap, indirect and direct transitions, from 3.50 and 4.80, 3.70 and 4.87, 3.80 and 4.88, 3.6 and 4.70, and, 3.50 and 4.80 eV to 3.25 and 4.65, 3.50 and 4.75, 3.65 and 4.76, 3.45 and 4.65 as well as 3.25 and 4.60 eV for annealed/alpha-irradiated PADC films annealed at 120 °C for 2, 4, 6, 8, and 10 h, respectively. The phonon energy, the Urbach energy and the number of carbon atoms (N) per conjugated length in the annealed/exposed PADC films remained constant for each annealing period, and showed an opposite effect compared with the un-annealed, exposed films.

(3) The material of the thermally treated PADC film-based NTDs was demonstrated to be insensitive to particles with lower ionization rates (such as alpha particles).

(4) The current observations suggested that the PADC polymer enabled an estimated alpha particle dose to be determined.

Acknowledgments

We would like to thank Dr. Ahmad Mami, the Dean of our Faculty, for his encouragement and assistance. We also acknowledge Dr. Ali Y. Darkwi, the Head of the Physics Department, and Dr. Ibrahim M. Hamammu, the Director of Postgraduate Studies, for their encouragement and facilities.

References

Abel, F., Quillet, V., Schott, M., 1995. Degradation of polystyrene thin films under d, ^{4}He and ^{12}C irradiation studied by ion beam analysis: effects of energy loss, sample thickness and isotopic content. Nucl. Instrum. Methods Phys. Res. B 105, 86–90.

AbouEl-Khier, A.A., Gaber, M., Mahmoud, S.A., El-Shafey, E., 1995. The effect of environmental treatment on the track response of the CR-39 plastic detector. Mater. Lett. 24, 41–45.

Anupam, Kumar, S., 1997. On the effect of cure cycle parameters and dopants on pre and post irradiation annealing response of CR-39 track detectors. Radiat. Meas 28, 181–184.

Calcagno, L., Compagnini, G., Foti, G., 1992. Structural modification of polymer films by ion irradiation. Nucl. Instrum. Methods Phys. Res. B 65, 413–422.

Cartwright, B.G., Shirk, E.K., Price, P.B, 1978. A nuclear-track-recording polymer of unique sensitivity and resolution. Nucl. Instrum. Methods 153, 457–460.

Cassou, R.M., Benton, E.V., 1978. Properties and applications of CR-39 polymeric nuclear track detector. Nucl. Track Detect 2, 173–179.

Durrani, S.A., Bull, R.K., 1987. Solid State Nuclear Track Detection: Principles and Applications. Pergamon Press, Oxford.

Durrani, S.A., Karamoust, N.A., Al-Khalifa, I.J.M., 1990. The Effect of the registration temperature on the response of CR-39 to alpha particles and fission fragments. Radiat. Protect. Dosimetry 34, 43–46.

Fink, D., Chung, W.H., Klett, R., Schmoldt, A., Cardoso, J., Montiel, R., Vazquez, M.H., Wang, L., Hosoi, F., Omichi, H., Goppelt-Langer, P., 1995. Carbonaceous clusters in irradiated polymers as revealed by UV–vis spectrometry. Radiat. Eff. Defects Solids 133, 193–208.

Fleischer, R.L., Price, P.B., 1963. Tracks of charged particles in high polymers. Science 140, 1221–1222.

Fleischer, R.L., Price, P.B., Symes, E.M., Miller, D.S., 1964. Fission track ages and track-annealing behavior of some micas. Science 143, 349–351.

Fleischer, R.L., Price, P.B., Walker, R.M, 1975. Nuclear Tracks in Solids: Principles and Application. University of California Press, Berkeley, USA.

Fox, Mark, 2001. Optical Properties of Solids. Oxford University Press Inc., New York.

Ipe, N.E., Ziemer, P.L., 1986. Effect of annealing on track density in unirradiated and gamma irradiated CR-39 when used for fast neutron detection. Nucl. Tracks Radiat. Meas 11, 137–140.

Jain, R.K., Rhandhawa, G.S., Rose, S.K., Virk, H.S., 1998. Study of etching and annealing characteristics of ^{238}U ion tracks in Trifol-TN polycarbonate. J. Phys. D: Appl. Phys 31, 328.

Jain, R.K., Kumar, A., Singh, B.K., 2012. Track etch parameters and annealing kinetics assessment of protons of low energy in CR-39 detector. Nucl. Instrum. Methods Phys. Res. B 274, 100–104.

Khan, E.U., Malik, F., Qureshi, I.E., Husaini, S.N., Ali, N., Mehmood, A., 2005. Measurement of neutron fluence with CR-39 using a UV spectrophotometer. Radiat. Meas. 40, 583–586.

Kumar, V., Sonkawade, R.G., Dhaliwal, A.S., 2010. Optimization of CR-39 as neutron dosimeter. Indian J. Pure Appl. Phys. 48, 466–469.

Kumar, V., Sonkawade, R.G., Chakarvarti, S.K., Kulriya, P., Kant, K., Singh, N.L., Dhaliwal, A.S., 2011. Study of optical, structural and chemical properties of neutron irradiated PADC film. Vacuum 86, 275–279.

Lounis-Mokrani, Z., Fromm, M., Barillon, R., Chambaudet, A., Allab, M., 2003. Characterization of chemical and optical modifications induced by 22.5 MeV proton beams in CR-39 detectors. Radiat. Meas. 36, 615–620.

Marletta, G., 1990. Chemical reactions and physical property modifications induced by keV ion beams in polymers. Nucl. Instrum. Methods Phys. Res. B 46, 295–305.

Modgil, S.K., Virk, H.S., 1985. Annealing of fission fragment tracks in inorganic solids. Nucl. Instrum. Methods Phys. Res. B 12, 212–218.

Mott, N.F., Davies, E.A., 1979. Electronic Processes in Non-Crystalline Materials. Clarendon Press, Oxford.

Phukan, T., Kanjilal, D., Goswami, T.D., Das, H.L., 2003. Study of optical properties of swift heavy ion irradiated PADC polymer. Radiat. Meas. 36, 611–614.

Raghuvanshi, S.K., Ahmad, B., Siddhartha, Srivastava, A.K., Krishna, J.B.M., Wahab, M.A., 2012. Effect of gamma irradiation on the optical properties of UHMWPE (ultra-high-molecular-weight-polyethylene) polymer. Nucl. Instrum. Methods Phys. Res. B 271, 44–47.

Rana, M.A., 2012. Mechanisms and kinetics of nuclear track etching and annealing: Free energy analysis of damage in fission fragment tracks. Nucl. Instrum. Methods Phys. Res. A 672, 57–63.

Rana, M.A., Qureshi, I.E., Khan, E.U., Manzoor, S., Shahzad, M.I., Khan, H.A., 2000. Thermal annealing of fission fragment radiation damage in CR-39. Nucl. Instrum. Methods Phys. Res. B 170, 149–155.

Saad, A.F., Atwa, S.T., Yokota, R., Fujii, M., 2005. Radiation-induced modifications on spectroscopic and thermal properties of CR-39 and SR-90 nuclear track detectors. Radiat. Meas. 40, 780–784.

Saad, A.F., El-Namrouty, A.A., Solyman, S., Atwa, S.T., 2011. Scanning Aged CR-39 SSNTDs with etched alpha tracks by using transmitted laser light. J. Korean Phys. Soc. 58, 701–705.

Saad, A.F., Hamed, N.A., Abdalla, Y.K., Tawati, D.M., 2012. Modifications of the registration properties of charged particles in a CR-39 polymeric track detector induced by thermal annealing. Nucl. Instrum. Methods Phys B 287, 60–67.

Saha, A., Chakraborty, V., Chintalapudi, S.N., 2000. Chemical modification of polypropylene induced by high energy carbon ions. Nucl. Instrum. Methods Phys. Res. B 168, 245–251.

Salamon, M.H., Price, P.B., Drach, J., 1986. Thermal annealing of nuclear tracks in polycarbonate plastic. Nucl. Instrum. Methods Phys. Res. B 17, 173–176.

Sharma, T., Aggarwal, S., Kumar, S., Mittal, V.K., Kalsi, P.C., Manchanda, V.K., 2007. Effect of gamma irradiation on the optical properties of CR-39 polymer. J. Mater. Sci 42, 1127–1130.

Urbach, F., 1953. The long-wavelength edge of photographic sensitivity and of the electronic absorption of solids. Phys. Rev. 92, 1324.
Yamauchi, T., Yasuda, N., Asuka, T., Izumi, K., Masutani, T., Oda, K., Barillon, R., 2005. Track core size estimation for heavy ions in CR-39 by AFM and UV methods. Nucl. Instrum. Methods Phys. Res. B 236, 318–322.
Young, D.A., 1958. Etching of radiation damage in lithium fluoride. Nature 182, 375–377.
Zaki, M.F., 2008. Gamma-induced modification on optical band gap of CR-39 SSNTD. J. Phys. D: Appl. Phys 41, 175404.